Encapsulating Bis(β-Ketoiminato) Polyethers. Volatile, Fluorine-Free Barium Precursors for Metal−Organic Chemical Vapor Deposition

Daniel B. Studebaker, Deborah A. Neumayer, Bruce J. Hinds, Charlotte L. Stern, and Tobin J. Marks*

Department of Chemistry, Materials Research Center, and Science and Technology Center for Superconductivity, Northwestern University, Evanston, Illinois 60208-3113

Received October 1, 1999

The synthesis, characterization, and incorporation in volatile metal−organic chemical vapor deposition (MOCVD) precursors of a new class of linked β-ketoiminate−polyether−β-ketoiminate ligands is presented. These ligands are designed to encapsulate alkaline-earth cations having low charges and large ionic radii. Barium complexes having the general formula Ba[(RCOCHC(R′)N)$_2$(R″)] (R = *tert*-butyl or CF_3; R′ = *tert*-butyl, methyl, or CF_3; R″ = $-(CH_2CH_2O)_4CH_2CH_2-$ or $-(CH_2CH_2O)_5CH_2CH_2)-$) were prepared and characterized by ^{1}H and ^{13}C NMR spectroscopy, elemental analysis, and mass spectrometry. Single-crystal X-ray diffraction analysis of 2,2,5,25,28,28-hexamethyl-9,12,15,18,21-pentaoxa-4,25-diene-6,24-diimino-3,27-pentacosadionatobarium(II) reveals a monomeric, nine-coordinate, tricapped trigonal prismatic coordination geometry. Single-crystal X-ray structural analysis of 1,1,1,24,24,24-hexafluoro-4,21-ditrifluoromethyl-8,11,14,17-tetraoxa-3,21-diene-5,20-diimino-2,23-tetracosadionatobarium(II)·2DMSO reveals a monomeric, ten-coordinate, distorted tetracapped trigonal prismatic coordination geometry. Volatility data are presented for these barium complexes, demonstrating viability as MOCVD precursors. In addition, it is demonstrated that thin epitaxial films of $BaTiO_3$ can be grown on (001) MgO by low-pressure MOCVD techniques using one of these barium complexes and Ti(dipivaloylmethanate)$_2$(isopropoxide)$_2$ as precursors.

Introduction

Metal−organic chemical vapor deposition (MOCVD) is the process of choice for the growth of ceramic thin films for numerous solid-state electronic devices.[1] Large-scale film growth by MOCVD takes advantage of simpler, less costly equipment, ready scalability, and higher throughput as compared to conventional physical vapor deposition (PVD) techniques. Furthermore, MOCVD produces conformal coatings over steps, vias, and other surface topographies, in contrast to PVD which is a line-of-sight technique. Sol−gel processing, a less expensive film growth technique, can suffer from voids, poor control of film thickness and smoothness, and carbon contamination. Therefore, MOCVD is widely used to reproducibly grow high-quality thin films for a wide spectrum of applications. Critical to the efficiency of any MOCVD process are the properties of the metal−organic precursors. These species must be volatile, exhibit stable vapor pressures, and cleanly decompose to the desired product at useful substrate temperatures.[1c,d,f] Many compounds which satisfy the above criteria are used to produce high-quality thin films containing the respective metal centers. Unfortunately barium, critical to high-temperature superconductors[2] such as $YBa_2Cu_3O_{7-x}$ and $Tl_2Ba_2CaCu_2O_{7-x}$, ferroelectrics[3] such as $BaTiO_3$ and $(Ba_{1-x}Sr_x)TiO_3$, nonlinear optical materials[4] such as β-BaB_2O_4, and collosal magnetoresistive materials[5] such as $La_{0.66}Ba_{0.33}MnO_3$, does not currently have a molecular precursor which conforms to all of the above requirements. Although MOCVD growth of the above materials has been successfully accomplished with varying degrees of success using known barium complexes,[6] current generation precursors exhibit significant deficiencies.[7] Thus, while homoleptic β-diketonates of group II and transition elements are often useful precursors, the simple β-diketonates of Ba^{2+} are typically oligomeric because of the low Ba^{2+} ionic charge:radius ratio.[8] This tendency for oligomerization substantially reduces molecular volatility. Monomeric barium β-diketonates can be formed by saturating the metal coordination sphere with polydentate neutral Lewis base functionalities such as tetraglyme (tetraethylene glycol dimethyl ether). However, when tetraglyme is coordinated to barium(II) β-diketonates having nonfluorinated ligands such as Ba(dpm)$_2$ (dpm = dipivaloylmethanate) (Figure 1A), the ensuing complex (Figure 1B) readily loses tetraglyme upon attempted

* To whom correspondence should be addressed at the Department of Chemistry.

(1) (a) Neumuller, H.-W.; Schmidt, W.; Kinder, H.; Freyhardt, H. C.; Stritzker, B.; Wordenweber, R.; Kirchhoff, V. *J. Alloys Compd.* **1997**, *251*, 366. (b) Kodas, T.; Hampden-Smith, M. *The Chemistry of Metal CVD*; VCH Publishers: Weinheim, Germany, 1994. (c) Pierson, H. O. *Handbook of Chemical Vapor Deposition*; Noyes: Park Ridge, NJ, 1992. (d) Morosanu, C. E. *Thin Films by Chemical Vapour Deposition*; Elsevier: Amsterdam, 1990. (e) Kern, W.; Ban, V. S. In *Thin Film Processes*; Kern, W., Vossen, J. L., Eds.; Academic Press: New York, 1978. (f) Dapkus, P. D.; Coleman, J. J. In *Materials Processing-Theory and Practices*; Malik, R. J., Ed.; North-Holland: Amsterdam, 1989.

(2) Leskela, M.; Molsa, H.; Niinisto, L. *Supercond. Sci. Technol.* **1993**, *6*, 627.

(3) (a) Dimos, D. *Annu. Rev. Mater. Sci.* **1995**, *25*, 273. (b) Kaiser, D. L.; Vaudin, M. D.; Gillen, G.; Hwang, C. S.; Robbins, L. H.; Rotter, L. D. J. *Cryst. Growth* **1994**, *137*, 136. (c) Chen, J.; Wills, L. A.; Wessels, B. W.; Schulz, D. L.; Marks, T. J. *J. Electron. Mater.* **1993**, *22*, 701. (d) Van Buskirk, P. C.; Gardiner, R.; Kirlin, P. S.; Nutt, S. *J. Mater. Res.* **1992**, *7*, 542.

(4) (a) Lin, J. T. *Opt. Quantum Electron.* **1990**, *22*, S283. (b) Eimerl, D.; Davis, L.; Velsko, S.; Graham, E. K.; Zalkin, A. *J. Appl. Phys.* **1987**, *62*, 1968.

(5) (a) Caignaert, V.; Millange, F.; Domenges, B.; Raveau, B. *Chem. Mater.* **1999**, *11*, 930. (b) von Helmolt, R.; Wecker, J.; Holzapfel, B.; Schultz, L.; Samwer, K. *Phys. Rev. Lett.* **1993**, *71*, 2331.

10.1021/ic991161a CCC: $19.00
Published on Web 06/28/2000

sublimation.[9] In contrast, if fluorinated β-diketonates such as hexafluoroacetylacetonate (hfa) are employed (Figure 1C), the coordinated tetraglyme does not undergo significant dissociation prior to or during sublimation, presumably reflecting the electron-withdrawing characteristics of the fluorine substituents and the resulting enhanced Lewis acidity of the Ba^{2+} center. Thus, $Ba(hfa)_2$·polyglyme compounds are volatile and have temporally stable vapor pressures; however, they do not decompose cleanly to oxide films at the substrate. Film growth with these fluorinated precursors generally requires either a postdeposition treatment of the film or use of water as a coreactant during film growth to reduce BaF_2 impurities.[6g,j,10] In this paper, we present an approach to fluorine-free barium MOCVD precursors in which β-ketonate ligands are modified to accommodate covalently linked polyether bridges, and thus

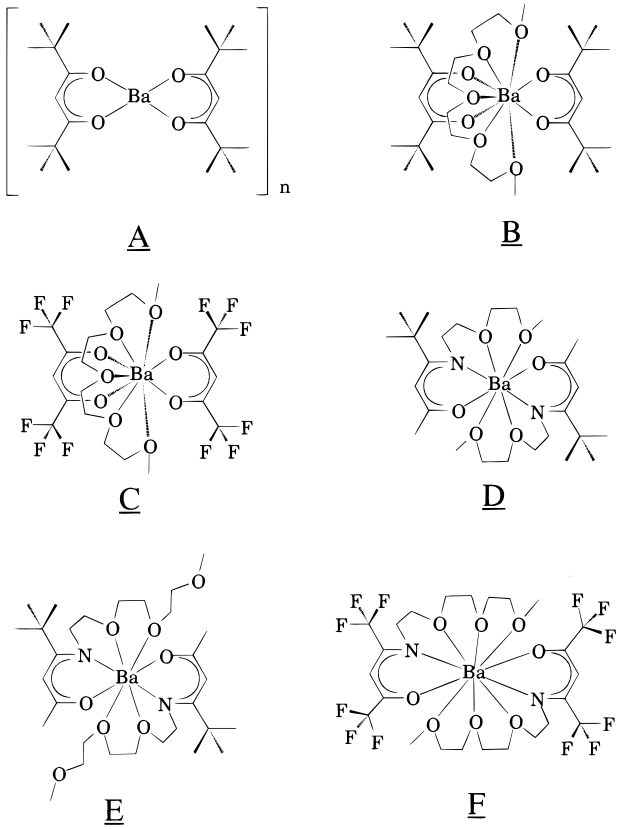

Figure 1. Molecular structures of the barium complexes discussed in the text: (A) $[Ba(dpm)_2]_n$, (B) Ba(dpm)2·tetraglyme, (C) $Ba(hfa)_2$·tetraglyme, (D) $Ba(diki)_2$, (E) $Ba(triki)_2$, (F) $Ba(hfatriki)_2$.

to address key instability characteristics inherent in the structures of Figure 1B.

Earlier work in this laboratory led to development of a new ligand system in which polyethelyene glycol units are covalently appended to nonfluorinated β-ketoiminate backbones.[7n,o] The goal of this strategy was to impede dissociation of the polyethlyene glycol ligand by covalently linking it to a modified β-diketonate which is also directly coordinated to the Ba^{2+} center. An example of this class of compounds is illustrated as compound **I** and in Figure 1D−F. Such precursors are volatile

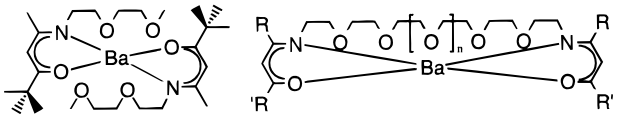

and can be used to grow oxide films; however, they sublime with significant thermal decomposition. The present study seeks to circumvent such decomposition pathways by covalently fusing the two β-diketonates via a polyether linkage. The intention is to neutralize the Ba^{2+} charge as well as to cloak the large metal coordination sphere in a single encapsulating, dianionic ligand. The general architecture of this ligand class is shown as compound **II** (R = $C(CH_3)_3$, CH_3, CF_3; R′ = $C(CH_3)_3$, CF_3; n = 0, 1).

Here we report the synthesis and structural characterization of five new encapsulating ligands of this type designed to coordinate metal ions having large radius:charge ratios such as the heavy alkaline earths. The reactivity of these ligands with Ba^{2+} and the volatility of the resulting complexes is examined. One of these barium precursors in combination with $Ti(^iOPr)_2$-

(6) (a) Burtman, V. *J. Mater. Sci. Lett.* **1998**, *17*, 1491. (b) Hinds, B. J.; McNeely, R. J.; Studebaker, D. B.; Marks, T. J.; Hogan, T. P.; Schindler, J. L.; Kannewurf, C. R.; Feng, X.; Miller, D. J. *J. Mater. Res.* **1997**, *12*, 1214−1236. (c) McNeely, R. J.; Belot, J. A.; Hinds, B. J.; Marks, T. J.; Schindler, J. L.; Chudzik, M. P.; Kannewurf, C. R.; Zhang, X. F.; Miller, D. J. *Appl. Phys. Lett.* **1997**, *71*, 1243. (d) Dahmen, K.-H.; Carris, M. W. *J. Alloys Compd.* **1997**, *251*, 270. (e) Yoshida, Y.; Ito, Y.; Hirabayash, I.; Nagai, H.; Takai, Y. *Appl. Phys. Lett.* **1996**, *69*, 845. (f) Zama, H.; Morishita, T. *Jpn. J. Appl. Phys., Lett.* **1996**, *35*, L770. (g) Hinds, B. J.; Studebaker, D. B.; Chen, J.; McNeely, R. J.; Han, B.; Schindler, J. L.; Hogan, T. P.; Kannewurf, C. R.; Marks, T. J. *J. Phys. IV* **1995**, *5*, C5, 391. (h) Wessels, B. W. *Annu. Rev. Mater. Sci.* **1995**, *25*, 525. (i) Dean, K. A.; Buchholz, D. B.; Marks, L. D.; Chang, R. P. H.; Vuchic, B. V.; Merkle, K. L.; Studebaker, D. B.; Marks, T. J. *J. Mater. Res.* **1995**, *10*, 2700. (j) Richards, B. C.; Cook, S. L.; Pinch, D. L.; Andrews, G. W.; Lengeling, G.; Schulte, B.; Jurgensen, H.; Shen, Y. Q.; Vase, P.; Freltoft, T.; Spee, C. I. M. A.; Linden, J. L.; Hitchman, M. L.; Shamlian, S. H.; Brown, A. *Physica C* **1995**, *252*, 229. (k) Schulz, D. L.; Marks, T. J. *Adv. Mater.* **1994**, *6*, 719. (l) Watson, I. M.; Atwood, M. P.; Cardwell, D.; Cumberbatch, T. J. *J. Mater. Chem.* **1994**, *4*, 1393.

(7) (a) Neumayer, D. A.; Belot, J. A.; Feezel, R. L.; Reedy, C.; Stern, C. L.; Marks, T. J.; Liable-Sands, L. M.; Rheingold, A. L. *Inorg. Chem.* **1998**, *37*, 5625−5633. (b) Belot, J. A.; Neumayer, D. A.; Reedy, C. A.; Studebaker, D. B.; Hinds B. J.; Stern, C. L., Marks, T. J. *Chem. Mater.* **1997**, *9*, 1638. (c) Otway, D. J.; Obi, B.; Rees, Jr., W. S. *J. Alloys Compd.* **1997**, *251*, 254. (d) Igumenov, I. K.; Semyannikov, P. P.; Belayas, S. V.; Zanina, A. S.; Shergina, S. I.; Sokolov, I. E. *Polyhedron* **1996**, *15*, 4521. (e) Motevalli, M.; Obrien, P.; Watson, I. M. *Polyhedron* **1996**, *15*, 1865. (f) Labrize, F.; Hubertpfalzgraf, L. G.; Daran, J. C.; Halut, S.; Tobaly, P. *Polyhedron* **1996**, *15*, 2707. (g) Marks, T. J. *Pure Appl. Chem.* **1995**, *67*, 313. (h) Aranasalam, V. C.; Baxter, I.; Drake, S. R.; Hursthouse, M. B.; Malik, K. M. A.; Otway, D. J. *Inorg. Chem.* **1995**, *34*, 5295. (i) Nash, J. A. P.; Thompson, S. C.; Foster, D. F.; Cole-Hamilton, D. J.; Barnes, J. C. *J. Chem. Soc., Dalton Trans.* **1995**, *2*, 269. (j) Neumayer, D. A.; Studebaker, D. B.; Hinds, B. J.; Stern, C. L.; Marks, T. J. *Chem. Mater.* **1994**, *6*, 878. (k) Herrmann, W. A.; Huber, N. W.; Priermeier, T. *Angew. Chem., Int. Ed. Engl.* **1994**, *33*, 105. (l) Burkey, D. J.; Williams, R. A.; Hanusa, T. P. *Organometallics* **1993**, *12*, 1331. (m) Sievers, R. E.; Turnipseed, S. B.; Huang, L.; Lagalante, A. F. *Coord. Chem. Rev.* **1993**, *128*, 285. (n) Schulz, D. L.; Hinds, B. J.; Neumayer, D. A.; Stern, C. L.; Marks, T. J. *Chem. Mater.* **1993**, *5*, 1605. (o) Schulz, D. L.; Hinds, B. J.; Stern, C. L.; Marks, T. J. *Inorg. Chem.* **1993**, *32*, 249. (p) Rees, W. S.; Caballero, C. R.; Hesse, W. *Angew. Chem., Int. Ed. Engl.* **1992**, *31*, 735.

(8) (a) Burtman, V.; Schieber, M.; Yitzchaik, S.; Yaroslavsky, Y. *J. Cryst. Growth* **1997**, *174*, 801. (a) Westerhausen, M.; Hartmann, M.; Schwarz, W. *Inorg. Chem.* **1996**, *35*, 2421. (b) Drozdov, A.; Troyanov, S. *J. Phys. IV* **1995**, *5*, C5, 373. (c) Huang, L.; Turnipseed, S. B.; Haltiwanger, R. C.; Barkley, R. M.; Seivers, R. E. *Inorg. Chem.* **1994**, *33*, 798. (d) Drake, S. R.; Hursthouse, M. B.; Abdul Malik, K. M.; Otway, D. J. *J. Chem. Soc., Dalton Trans.* **1993**, 2883. (e) Turnipseed, S. B.; Barkley, R. M.; Sievers, R. E. *Inorg. Chem.* **1991**, *30*, 1164. (f) Drozdov, A. A.; Trojanov, S. I. *Polyhedron* **1992**, *11*, 2877. (g) Rossetto, G.; Polo, A.; Benetollo, F.; Porchia, M.; Zanella, P. *Polyhedron* **1992**, *11*, 979. (h) Rees, W. R.; Carris, M. W.; Hesse, W. *Inorg. Chem.* **1991**, *30*, 4481.

(9) (a) Gardiner, R.; Brown, D. W.; Kirlin, P. S.; Rheingold, A. L. *Chem. Mater.* **1991**, *3*, 1053. (b) Gardiner, R. A.; Gordon, D. C.; Stauf, G. T.; Vaartstra, B. A.; Ostrander, R. L.; Rheingold, A. L. *Chem. Mater.* **1994**, *6*, 1967.

$(dpm)_2$ is then used to grow epitaxial $BaTiO_3$ thin films by an MOCVD process.

Experimental Section

General Procedures. Standard Schlenk techniques and a Vacuum Atmospheres nitrogen-filled glovebox were used in handling the ligands and Ba complexes. Benzene and heptane were dried over sodium and distilled immediately prior to use. ^{1}H, ^{13}C, and ^{19}F NMR spectra were recorded in dry deoxygenated $CDCl_3$, C_6D_6, or DMSO-d_6 on a Varian Gemini 300 instrument with a 5 mm broadband probe. Chemical shifts for the ^{1}H and ^{13}C spectra are referenced to solvent signals, while ^{19}F spectra are referenced to an external $CFCl_3$ sample. Electron impact mass spectra were obtained on a VG 70-250 SE spectrometer using an ionization potential of 70 eV with a temperature ramp rate of 20 °C/s from ambient to 200 °C. Liquids and solids were loaded into capillary tubes and introduced using a direct insertion probe. All mass spectra were calibrated using PCR perfluorokerosene 755. Elemental analyses was performed by G.D. Searle, Inc. (Skokie, IL) or Onieda Research Services (Whitesboro, NY). Precursor vapor pressure characteristics were evaluated using a TA Instruments STD 2960 simultaneous thermogravimetric−differential thermal analysis (TGA−DTA) instrument. Weight loss was measured as the sample was heated to 300 °C at 5 °C/min under an atmosphere of nitrogen flowing over open platinum sample pans. For vacuum sublimation rate measurements, the chamber was evacuated with a 14 cfm direct drive Fisher Maxima D16A vacuum pump, and the nitrogen carrier gas was adjusted via a needle valve to maintain a background pressure of 6.0 Torr, measured with an MKS 122AA capacitance manometer. Glassware used with silane derivatives was silanated[7n] by drying in a 120 °C oven for 1 h, rinsing the interior surfaces of the hot glass with hexamethyldisilizane, and evaporating the excess hexamethyldisilizane in an N_2 stream.

Reagents. The β-diketone, 2,2-dimethyl-3,5-hexanedione (Hdhd), was prepared according to the literature procedure,[11] while 2,2,6,6-tetramethyl-3,5-heptanedione (Hdpm) was obtained from Lancaster Synthesis, 1,1,1,5,5,5-hexafluoro-2,4-pentanedione (Hhfa) was obtained from Oakwood Products, BaH_2 (95% metals purity) was obtained from Strem, and all other reagents were obtained from Aldrich. Unless otherwise noted, commercial reagents were used as received. α,ω-Diamino polyethers were prepared by procedures described elsewhere[12,13] and were found to be sufficiently pure for subsequent syntheses.

Di-β-ketoimine Syntheses. Di-β-ketoimines derived from 2,2-dimethyl-3,5-hexanedione (Hdhd) were prepared by the condensation[14] of the β-diketone with the corresponding diamino ethers in benzene. Di-β-ketoimines derived from 2,2,6,6-tetramethyl-3,5-heptanedione (Hdpm) and 1,1,1,5,5,5-hexafluoro-2,4-pentanedione (Hhfa) were prepared by reaction of the appropriate diamino polyether[13] with the trimethylsilyl derivative of the β-diketone.[15]

Synthesis of 2,2,25,25-Tetramethyl-5,22-di-*tert*-butyl-9,12,15,18-tetraoxa-4,22-diene-6,21-diimino-3,24-hexacosadione [H_2(dpm)$_2$CAP-4, 1]. Under an inert atmosphere, 2.53 g (10.0 mmol) of triethylene glycol diamine was added to 7.35 g (29.0 mmol) of 2,2,6,6-tetramethyl-5-(trimethylsiloxy)hept-4-en-3-one in a 100 mL silanated flask. The yellow solution was then heated with stirring for 5 h at 105 °C. The volatile byproducts of the reaction were removed by distillation at 170 °C/0.3 Torr, leaving behind 2.69 g of product as a yellow-orange oil (47% yield). ^{1}H NMR (300 MHz, $CDCl_3$): δ 1.11 (s, 18H, NCC(CH_3)$_3$), 1.25 (s, 18H, OCC(CH_3)$_3$), 3.63 (m, 20H, CH_2), 5.28 (s, 2H, C*H*), 11.62 (br s, 2H, N*H*). ^{13}C NMR (75 MHz, $CDCl_3$): δ 27.30 [NCC(CH_3)$_3$], 28.28 [OCC(CH_3)$_3$], 35.08 [NCC(CH_3)$_3$], 40.78 [OCC(CH_3)$_3$], 44.32 [NCH_2], 69.43 [OCH_2], 69.56 [OCH_2], 69.68 [OCH_2], 69.84 [OCH_2], 85.53 [*C*H], 172.44 [*C*N], 202.38 [*C*O]. MS (EI, 70 eV, m/e^+; (fragment); H_2L = H_2(dpm)$_2$CAP-4), 569 (H_2L), 511 (HL − C_4H_9), 360 (H_2L − $CHCH_2NHC(C_4H_9)_2CHCO(C_4H_9)$) 328 ($H_2L$ − CH_2OCH_2-$CH_2NHC(C_4H_9)_2CHCO(C_4H_9)$), 210 ($CH_2CH_2NHC(C_4H_9)_2CHCO(C_4H_9)$), 151 ($C(C_4H_9)_2CHC(C_4H_9)$).

Synthesis of 2,2,28,28-Tetramethyl-5,25-di-*tert*-butyl-9,12,15,18,21-tetraoxa-4,25-diene-6,24-diimino-3,27-nanacosadione [H_2(dpm)$_2$CAP-5, 2]. Under an inert atmosphere, 1.58 g (5.60 mmol) of tetraethylene glycol diamine was added to 2.00 g (7.80 mmol) of 2,2,6,6-tetramethyl-5-(trimethylsiloxy)hept-4-en-3-one in a 100 mL silanated flask. The yellow solution was then heated with stirring for 5 h at 110 °C. The volatile byproducts of the reaction were removed by distillation at 120 °C/0.1 Torr, leaving behind 2.69 g of product as a yellow-orange oil (47% yield). ^{1}H NMR (300 MHz, $CDCl_3$): δ 1.11 (s, 18H, NCC(CH_3)$_3$), 1.25 (s, 18H, OCC(CH_3)$_3$), 3.64 (m, 24H, CH_2), 5.29 (s, 2H, C*H*), 11.61 (br s, 2H, N*H*). ^{13}C NMR (75 MHz, $CDCl_3$): δ 27.87 [NCC(CH_3)$_3$], 28.85 [OCC(CH_3)$_3$], 35.75 [NCC(CH_3)$_3$], 41.45 [OCC(CH_3)$_3$], 44.86 [NCH_2], 70.06 [OCH_2], 70.16 [OCH_2], 70.26 [OCH_2], 70.45 [OCH_2], 86.34 [*C*H], 173.34 [*C*N], 203.40 [*C*O]. MS (EI, 70 eV, m/e+; (fragment); H_2L = H_2(dpm)$_2$CAP-5), 612 (H_2L), 611 (HL), 555 (H_2L − C4H9), 404 (H_2L − $CCH_2NHC(C_4H_9)_2CHCO(C_4H_9)$), 372 ($H_2L$ − $CH_2OCH_2CH_2NHC(C_4H_9)_2CHCO(C_4H_9)$).

Synthesis of 2,2,5,22,25,25-Hexamethyl-9,12,15,18-tetraoxa-4,22-diene-6,21-diimino-3,24-hexacosadione [H_2(dhd)$_2$CAP-4, 3]. In a 100 mL reaction flask equipped with a Dean Stark trap and under an inert atmosphere, 5.00 g of triethylene glycol diamine (21.0 mmol) and 6.50 g of 2,2-dimethyl-3,5-hexanedione (46.0 mmol) were combined. To the flask were then added 75 mL of benzene and 30 drops of glacial acetic acid, and the mixture was allowed to reflux for 20 h. Benzene was then removed in vacuo, and the remaining liquid was distilled. The product distilled at 180 °C/0.8 Torr, yielding 8.02 g of product as a yellow oil (79% yield). ^{1}H NMR (300 MHz, $CDCl_3$): δ 1.09 (s, 18H, C(CH_3)$_3$), 1.94 (s, 6H, CCH_3), 3.40 (m, 4H, NCH_2), 3.60 (m, 16H, OCH_2), 5.10 (s, 2H, C*H*), 10.95 (br s, 2H, N*H*). ^{13}C NMR (75 MHz, $CDCl_3$): δ 18.86 [CCH_3], 27.35 [C(CH_3)$_3$], 40.51 [*C*(CH_3)$_3$], 42.31 [NCH_2], 69.64 [OCH_2], 69.83 [OCH_2], 69.95 [OCH_2], 70.06 [OCH_2], 90.01 [*C*H], 163.17 [*C*N], 202.84 [*C*O]. MS (EI, 70 eV, m/e^+; (fragment); H_2L = H_2(dhd)$_2$CAP-4), 485 (H_2L), 428 (H_2L − C_4H_9), 318 (H_2L − $CHCH_2NHCCH_3CHCOC_4H_9$).

Synthesis of 2,2,5,25,28,28-Hexamethyl-9,12,15,18,21-pentaoxa-4,25-diene-6,24-diimino-3,27-pentacosadione [H_2(dhd)$_2$CAP-5, 4]. In a 100 mL reaction flask equipped with a Dean Stark trap and under an inert atmosphere, 5.93 g of tetraethylene glycol diamine (21.0 mmol) and 6.53 g of 2,2-dimethyl-3,5-hexanedione (46.0 mmol) were combined. To the flask were then added 75 mL of benzene and 30 drops of glacial acetic acid, and the mixture was allowed to reflux for 20 h. Benzene was then removed in vacuo, and the remaining liquid was distilled. The product distilled at 180 °C/0.8 Torr, yielding 4.14 g of an orange oil (38% yield). ^{1}H NMR (300 MHz, $CDCl_3$): δ 1.09 (s, 18H, C(CH_3)$_3$), 1.94 (s, 6H, CCH_3), 3.39 (m, 4H, NCH_2), 3.61 (m, 20H, OCH_2), 5.10 (s, 2H, C*H*), 10.95 (br s, 2H, N*H*). ^{13}C NMR (75 MHz, $CDCl_3$): δ 19.16 [CCH_3], 27.61 [C(CH_3)$_3$], 40.84 [*C*(CH_3)$_3$], 42.61 [NCH_2], 69.95 [OCH_2], 70.18 [OCH_2], 70.37 [OCH_2], 90.33 [*C*H], 163.44 [*C*N], 203.31 [*C*O]. MS (EI, 70 eV, m/e^+; (fragment); H_2L = H_2(dhd)$_2$CAP-5), 529 (H_2L), 527 (L), 470 (L − C_4H_9), 360 (H_2L − $CHCH_2NHCCH_3CHCOC_4H_9$), 303 (H_2L − C_4H_9 − $CHCH_2$-$NHCCH_3CHCOC_4H_9$).

Synthesis of 1,1,1,24,24,24-Hexafluoro-4,21-ditrifluoromethyl-8,-11,14,17-tetraoxa-3,21-diene-5,20-diimino-2,23-tetracosanedione [H_2(hfa)$_2$CAP-4, 5]. Under an inert atmosphere, 2.04 g (8.60 mmol) of triethylene glycol diamine was added to 5.95 g (21.0 mmol) of 3-ene-1,1,1,5,5,5-hexafluoro-4-trimethylsiloxy-2-pentanone in a 100 mL silanated flask. The solution was stirred for 30 min, and the ligand was then distilled at 135 °C/0.3 Torr, yielding 3.57 g of an orange oil (67% yield). ^{1}H NMR (300 MHz, $CDCl_3$): δ 3.63 (m, 20H, CH_2), 5.78 (s, 2H, C*H*), 10.64 (br s, 2H, N*H*). ^{13}C NMR (75 MHz, $CDCl_3$): δ 44.45 [NCH_2], 68.29 [OCH_2], 70.11 [OCH_2], 70.20 [OCH_2], 70.34 [OCH_2], 85.76 [*C*H], 116.48 [NC*C*F_3], 118.96 [OC*C*F_3], 153.47 [*C*N], 279.23 [*C*O]. ^{19}F (282 MHz, $CDCl_3$): δ −77.82 [OCC*F*$_3$], −67.79

(10) (a) Shamlian, S. K.; Hitchman, M. L.; Cook, S. L.; Richards, B. C. *J. Mater. Chem.* **1994**, *4*, 81. (b) Zhao, J.; Marcy, H. O.; Tonge, L. M.; Wessels, B. W.; Marks, T. J.; Kannewurf, C. R. *Physica C* **1994**, *159*, 710.
(11) Swarmer, F. W.; Hauser, C. R. *J. Am. Chem. Soc.* **1950**, *72*, 1352.
(12) Dale, J.; Kristiansen, P. O. *Acta Chem. Scand.* **1972**, *26*, 1471.
(13) Kern, W.; Iwabuchi, S.; Sato, H.; Bohmer, V. *Makromol. Chem.* **1979**, *180*, 2539.
(14) Moffett, R. B.; Hoehn, W. M. *J. Am. Chem. Soc.* **1947**, *69*, 1792.
(15) Shin, H.-K.; Hampden-Smith, M. J.; Kodas, T. T.; Rheingold, A. L. *J. Chem. Soc., Chem. Commun.* **1992**, 217.

[NCCF_3]. MS (EI, 70 eV, m/e^+; (fragment); $H_2L = H_2(CF_3-CF_3)_2$CAP-4), 616 (H_2L), 597 ($H_2L - F$), 385 ($H_2L - CHCH_2NC(C_4F_9)_2CHCO(C_4F_9)$).

Barium Di-β-ketoiminate Syntheses. The barium di-β-ketoimine complexes were prepared by reacting the neat ligand with BaH_2 in excess,[7n] as described below.

Synthesis of 2,2,25,25-Tetramethyl-5,22-di-*tert*-butyl-9,12,15,18-tetraoxa-4,22-diene-6,21-diimino-3,24-hexacosadionatobarium(II) [Ba(dpm)$_2$CAP-4, 6]. In a 100 mL reaction flask under an inert atmosphere, 1.27 g (2.20 mmol) of $H_2(dpm)_2$CAP-4 was added to 1.88 g (14.0 mmol) of BaH_2. The mixture was heated with stirring at 105 °C for 48 h. Dry THF (50 mL) was then added, the mixture brought to reflux, and the solution filtered while hot to remove unreacted solid BaH_2. The solvent was then removed from the filtrate in vacuo, and the solid product was sublimed at 70 °C/10^{-5} Torr, yielding 0.21 g of a white solid (14% yield). ^{1}H NMR (300 MHz, C_6D_6): δ 1.12 (s, 18H, NCC(CH_3)$_3$), 1.25 (s, 18H, OCC(CH_3)$_3$), 3.64 (m, 20H, CH_2), 5.29 (s, 2H, C*H*). ^{13}C NMR (75 MHz, C_6D_6): δ 28.51 [NCC(*C*H$_3$)$_3$], 29.32 [OCC(*C*H$_3$)$_3$], 35.62 [NC*C*(CH$_3$)$_3$], 41.02 [OC*C*(CH$_3$)$_3$], 43.12 [N*C*H$_2$], 68.90 [O*C*H$_2$], 69.23 [O*C*H$_2$], 69.41 [O*C*H$_2$], 69.72 [O*C*H$_2$], 86.38 [*C*H], 174.29 [*C*N], 198.77 [*C*O]. Anal. Calcd for $C_{32}H_{58}N_2O_6Ba$: C, 54.58; H, 8.30; N, 3.98. Found: C, 53.81; H, 8.21; N, 4.01. MS (EI, 70 eV, m/e^+; (fragment); M = Ba(dpm)$_2$CAP-4), 704 (M), 496 (M − $CHCH_2NC(C_4H_9)_2CHCO(C_4H_9)$), 452 (M − $CHCH_2OCH_2CH_2NC(C_4H_9)_2CHCO(C_4H_9)$).

Synthesis of 2,2,5,22,25,25-Hexamethyl-9,12,15,18-tetraoxa-4,22-diene-6,21-diimino-3,24-hexacosadionatobarium(II) [Ba(dhd)$_2$CAP-4, 7]. In a 100 mL reaction flask under inert atmosphere, 1.23 g (2.50 mmol) of $H_2(dhd)_2$CAP-4 was added to 1.03 g (7.40 mmol) of BaH_2. The mixture was heated with stirring at 120 °C for 30 min. Dry THF (50 mL) was then added, the mixture heated to reflux, and the solution filtered while hot to remove unreacted solid BaH_2. The solvent was then removed from the filtrate, yielding 0.15 g of a white solid (10% yield). ^{1}H NMR (300 MHz, C_6D_6): δ 1.10 (s, 18H, C(CH_3)$_3$), 1.95 (s, 6H, CCH_3), 3.41 (m, 4H, NCH_2), 3.60 (m, 16H, OCH_2), 5.11 (s, 2H, C*H*). ^{13}C NMR (75 MHz, C_6D_6): δ 19.17 [C*C*H$_3$], 27.85 [C(*C*H$_3$)$_3$], 40.65 [*C*(CH$_3$)$_3$], 42.26 [N*C*H$_2$], 69.25 [O*C*H$_2$], 69.63 [O*C*H$_2$], 69.77 [O*C*H$_2$], 69.88 [O*C*H$_2$], 89.61 [*C*H], 163.42 [*C*N], 201.44 [*C*O]. Anal. Calcd for $C_{26}H_{46}N_2O_6Ba$: C, 50.32; H, 7.42; N, 4.52. Found: C, 51.02; H, 7.70; N, 4.65. MS (EI, 70 eV, m/e^+; (fragment); M = Ba(dhd)$_2$CAP-4), 620 (M), 454 (M − $CHCH_2NCCH_3CHCOC_4H_9$), 424 (M − $CHOCH_2CH_2NCCH_3CHCOC_4H_9$).

Synthesis of 2,2,5,25,28,28-Hexamethyl-9,12,15,18,21-pentaoxa-4,25-diene-6,24-diimino-3,27-pentacosadionatobarium(II) [Ba(dhd)$_2$-CAP-5, 8]. In a 100 mL reaction flask under an inert atmosphere, 2.65 g (5.00 mmol) of $H_2(dhd)_2$CAP-5 was added to 1.65 g (12.0 mmol) of BaH_2. The mixture was heated with stirring at 110 °C for 30 min. Freshly distilled heptane was then added, the mixture brought to reflux, and the solution filtered while hot to remove unreacted solid BaH_2. The filtration step was repeated three times. The desired complex crystallized from the combined filtrates after standing at room temperature for 24 h, yielding 2.13 g of colorless crystals (64% yield). The solid can be further purified by sublimation at 140 °C/10^{-5} Torr. ^{1}H NMR (300 MHz, C_6D_6): δ 1.10 (s, 18H, C(CH_3)$_3$), 1.95 (s, 6H, CCH_3), 3.40 (m, 4H, NCH_2), 3.60 (m, 20H, OCH_2), 5.11 (s, 2H, C*H*). ^{13}C NMR (75 MHz, C_6D_6): δ 21.64 [C*C*H$_3$], 30.38 [C(*C*H$_3$)$_3$], 40.08 [*C*(CH$_3$)$_3$], 48.76 [N*C*H$_2$], 68.76 [O*C*H$_2$], 69.84 [O*C*H$_2$], 70.33 [O*C*H$_2$], 70.50 [O*C*H$_2$], 72.76 [O*C*H$_2$], 91.56 [*C*H], 165.80 [*C*N], 186.28 [*C*O]. Anal. Calcd for $C_{28}H_{50}N_2O_7Ba$: C, 50.60; H, 7.53; N, 4.22. Found: C, 50.67; H, 7.40; N, 4.01. MS (EI, 70 eV, m/e^+; (fragment); M = Ba(dhd)$_2$CAP-5), 664 (M), 498 (M − $CHCH_2NCCH_3CHCOC_4H_9$), 471 (M − $2CCOC_4H_9$).

Synthesis of 1,1,1,24,24,24-Hexafluoro-4,21-ditrifluoromethyl-8,11,14,17-tetraoxa-3,21-diene-5,20-diimino-2,23-tetracosanedionatobarium(II) [Ba(hfa)$_2$CAP-4, 9]. In a 100 mL reaction flask under an inert atmosphere, 3.50 g (5.70 mmol) of $H_2(hfa)_2$CAP-4 was added to 1.40 g (10.0 mmol) of BaH_2. To the ensuing peach-colored mixture was added 50 mL of dry THF, the mixture brought to reflux for 30 min., and the solution filtered while hot to remove unreacted solid BaH_2. The solvent was then removed from the filtrate, affording colorless, needlelike crystals. The solid was sublimed at 215 °C/10^{-5} Torr, yielding 1.11 g of a colorless solid (26% yield). ^{1}H NMR (300 MHz, DMSO-d_6): δ 3.71 (m, 20H, CH_2), 5.41 (s, 2H, C*H*). ^{13}C NMR (75 MHz, DMSO-d_6): δ 43.86 [N*C*H$_2$], 67.94 [O*C*H$_2$], 69.05 [O*C*H$_2$], 69.33 [O*C*H$_2$], 69.61 [O*C*H$_2$], 86.07 [*C*H], 116.90 [NC*C*F$_3$], 119.43 [OC*C*F$_3$], 154.22 [*C*N], 278.80 [*C*O]. ^{19}F (282 MHz, DMSO-d_6): δ −75.21 [OCC*F*$_3$], −65.22 [NCC*F*$_3$]. Anal. Calcd for $C_{20}H_{22}N_2O_6F_{12}Ba$: C, 31.96; H, 2.95; N, 3.73. Found: C, 32.39; H, 2.89; N, 3.53. MS (EI, 70 eV, m/e^+; (fragment); M = Ba(CF$_3$−CF$_3$)$_2$CAP-4) 751 (M), 732 (M − F), 713 (M − 2F), 519 (M − $CHCH_2NC(C_4F_9)_2CHCO(C_4F_9)$), 444 (M − $CH(OCH_2CH_2)_2NC(C_4F_9)_2CHCO(C_4F_9)$), 400 (M − $CH(OCH_2CH_2)_3NC(C_4F_9)_2CHCO(C_4F_9)$), 273 (Ba + NC(C$_4F_9$)CHCO), 156 (BaF).

Table 1. Crystal Data and Diffraction Experimental Details for **8** and **9**·2DMSO

	8	**9**·2DMSO
empirical formula	$BaC_{28}H_{50}O_7N_2$	$BaC_{24}H_{34}O_8N_2F_{12}S_2$
fw	664.04	907.97
space group	$P2_1/c$ (no. 14)	$C2/c$ (no. 15)
a, Å	11.843(3)	23.179(4)
b, Å	15.782(3)	8.806(4)
c, Å	17.836(5)	18.381(4)
β, deg	108.39(2)	111.55(2)
V, Å^3	3163(1)	3489(1)
Z	4	4
d_{calcd}, g/cm^3	1.39	1.73
temp, °C	−120 ± 1	−120 ± 1
λ(Mo Kα) radiation, Å	0.170 69	0.170 69
μ, cm^{-1}	13.0	13.7
transm factors	0.78−0.91	0.67−0.83
R^a	0.040	0.031
$R_w{}^b$	0.033	0.036

^{a} $R = \sum||F_o| - |F_c||/\sum|F_o|$. ^{b} $R_w = [(\sum w(|F_o| - |F_c|)^2/\sum wF_o^2)]^{1/2}$

Single-Crystal X-ray Diffraction Studies. X-ray data for single crystals of Ba(dhd)$_2$CAP-5 (**8**) and [Ba(hfa)$_2$CAP-4]·2DMSO (**9**·2DMSO) were collected on an Enraf-Nonius CAD4 with graphite-monochromated Mo Kα radiation. A light yellow, transparent platey crystal of **8** having approximate dimensions of 0.22 × 0.21 × 0.08 mm was grown by slow evaporation from a saturated heptane solution and mounted on a glass fiber using oil (Paratone-N, Exxon). A colorless, transparent prismatic crystal of **9**·2DMSO having approximate dimensions of 0.51 × 0.26 × 0.14 mm was grown by slow cooling of a DMSO solution and similarly mounted. For **8** and **9**, cell constants and orientation matrices for data collection were obtained from a least-squares refinement using the setting angles of 25 carefully centered reflections in the range of 19.6° < 2θ < 24.1° and 14.0° < 2θ < 20.7°, respectively. These corresponded to primitive monoclinic and C-centered monoclinic cells with the dimensions listed in Table 1. The following systematic absences were observed for **8** and **9**·2DMSO, respectively: *h*0*l* ($l \neq 2n$) and 0*k*0 ($k \neq 2n$); and *hkl* ($h + k \neq 2n$) and *h*0*l* ($l \neq 2n$). On the basis of packing considerations, a statistical analysis of intensity distribution, and the successful solution and refinement of the structure, the space group of **9**·2DMSO was determined to be $C2/c$ (no. 15). The space group of **8** was unambiguously determined to be $P2_1/c$ by systematic absences.

Diffraction data for **8** and **9**·2DMSO were collected at a temperature of −120 ± 1 °C using the $\omega-\theta$ scan technique to maximum 2θ values of 49.9° and 53.9°, respectively. ω-scans of several intense reflections, made prior to data collection, had average widths at half-height of 0.03° and 0.25° for **8** and **9**·2DMSO, respectively, with a takeoff angle of 2.8°. Scans of (1.00 + 0.35 tan θ)° were made at variable speeds from 3 to 16 deg/min (in omega). Moving-crystal moving counter background measurements were made by scanning an additional 25% above and below the scan range. The counter aperture consisted of a variable horizontal slit with a width ranging from 2.0 to 2.5 mm and a vertical slit set to 2.0 mm. The diameter of the incident beam collimator was 0.7 mm, and the crystal-to-detector distance was 21 cm. For intense reflections, an attenuator was automatically inserted in front of the detector.

Of the 5981 and 4173 reflections which were collected for **8** and **9**·2DMSO, respectively, 5790 (R_{int} = 0.040) and 4063 (R_{int} = 0.024),

respectively, were unique. The intensities of three representative reflections, measured after every 90 min of X-ray exposure time, remained constant throughout data collection, indicating crystal and electronic stability (no decay correction was applied). The linear absorption coefficients for Mo Kα radiation were 13.0 and 13.7 cm^{-1} for **8** and **9**·2DMSO, respectively. An analytical absorption correction was applied which resulted in transmission factors ranging from 0.78 to 0.91 for **8**, and from 0.67 to 0.83 for **9**·2DMSO. The data were corrected for Lorentz and polarization effects. A correction for secondary extinction was applied for **9**·2DMSO (coefficient = 1.21976E−07).

The structures were solved (SHELXS-86) and expanded using Fourier techniques (DIRDIF92).[16] The disordered sulfur atoms in **9**·2DMSO were refined isotropically, with the occupancy of S1a refining to 0.62. The remaining non-hydrogen atoms for **9**·2DMSO and all non-hydrogen atoms for **8** were refined anisotropically. Hydrogen atoms were included in fixed positions and not refined for **8**, and were refined isotropically for **9**·2DMSO. The final cycle of full matrix least-squares refinement for **8** and **9**·2DMSO was based on 3461 and 3361 observed reflections ($I > 3.00\sigma(I)$) and 343 and 290 variable parameters, respectively. The refinements for **8** and **9**·2DMSO converged (the largest parameter shift was 0.01 and 0.65 times its esd, respectively) with unweighted and weighted agreement factors of $R = \sum||F_o| - |F_c||/\sum|F_o| = 0.040$ and 0.031 and $R_w = [(\sum w(|F_o| - |F_c|)^2/\sum wF_o^2)]^{1/2} = 0.033$ and 0.36, respectively. The standard deviation of an observed unit weight was 1.35 for **8** and 2.58 for **9**·2DMSO. The weighting scheme was based on counting statistics and included a factor ($p = 0.004$ for **8** and 0.009 for **9**·2DMSO) to downweight the intense reflections. Plots of $\sum w(|F_o| - |F_c|)^2$ versus $|F_o|$, reflection order in data collection, sin θ/λ, and various classes of indices showed no unusual trends. The maximum and minimum peaks on the final difference Fourier map corresponded to 0.62 and −0.71 $e^-/Å^3$ for **8** and 0.82 and −0.94 $e^-/Å^3$ for **9**·2DMSO.

Neutral atom scattering factors were taken from Cromer and Waber.[17] Anomolous dispersion effects were included in F_{calcd};[18] the values for $\Delta f'$ and $\Delta f''$ were those of Creagh and McAuley.[19] The values for the mass attenuation coefficients were those of Creagh and Hubbel.[20] All the calculations were performed using the TEXSAN crystallographic software package of Molecular Structure Corp.

MOCVD Film Growth Experiments and $BaTiO_3$ Film Characterization. Film growth was carried out in the inverted vertical MOCVD reactor described previously.[21] The barium source, Ba((dhd)$_2$CAP-5) (**8**), was placed in a boat which was maintained at 170 °C. A diglyme solution containing the titanium isopropoxide, Ti(dpm)$_2$(O^{i}Pr)$_2$, was transported to the reactor at ∼7 mmol/h by a liquid delivery system. The titanium-containing precursor solution was then "flash" vaporized, and transported to the substrate in a nitrogen carrier streamflowing at a rate of 200 sccm. The barium source was positioned downstream from the vaporization point and was not dissolved in a solvent. The oxidizer gases, oxygen and nitrous oxide, were introduced into the reactor at rates of 150 sccm, while the system base pressure was maintained at 0.85 Torr.

$BaTiO_3$ films were grown on cleaved single-crystal MgO (001) substrates which were degreased by sonication in a pentane solution and stored in a nitrogen atmosphere to avoid exposure to moisture. The films were deposited at a susceptor temperature of 830 °C. The susceptor temperature was measured with a thermocouple located at the center of the susceptor. However, a calibration study indicated that the temperature at the MgO surface is ∼200 °C lower than recorded. In the present study, a thermocouple was bonded to the surface of an MgO substrate with high-temperature cement. Measurements were taken under typical film growth conditions (low pressure, gas flow) to compare the surface temperature of the substrate with that recorded from the center of the susceptor. A difference in temperature of 4 °C was observed between the susceptor (120 °C) and the substrate surface (116 °C) at relatively low temperatures. At high temperatures, the difference increased to 175 °C (800 °C susceptor, 625 °C substrate surface).

Film growth was carried out for 1.0 h, and after deposition, the chamber was slowly backfilled with oxygen to atmospheric pressure, and the susceptor temperature reduced at 15 °C/min. $\theta-2\theta$ and rocking curve measurements were taken with a Rigaku D/Max-3HFX X-ray diffractometer using Ni-filtered Cu Kα radiation. The ϕ-scan data were obtained with a Troyke four-circle goniometer with Cu Kα radiation. Scanning electron microscopy was used to characterize the surface of the films using an ISI SEM instrument equipped with a Kevex EDX accessory to determine film stoichiometry.

Scheme 1. Di-β-ketoiminate Ligand Syntheses of 2,2,6,6-Tetramethyl-3,5-heptanedione and 1,1,1,5,5,5-Hexafluoro-4,2-pentanedione Derivatives

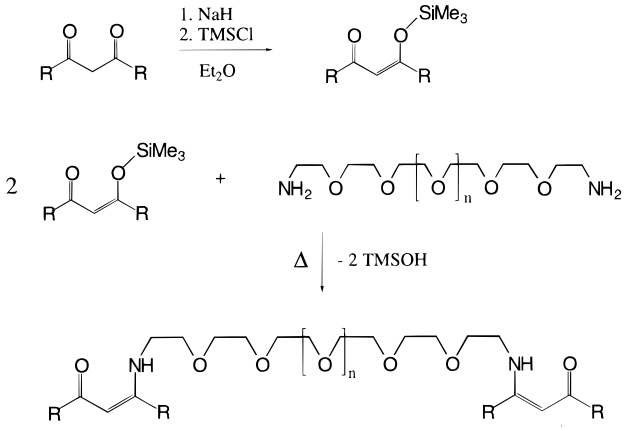

Ligand	R	n	Abbreviation
1	CH_3	0	H_2(dpm)$_2$CAP-4
2	CH_3	1	H_2(dpm)$_2$CAP-5
5	CF_3	0	H_2(hfa)$_2$CAP-4

Results and Discussion

Ligand and Complex Synthesis. The di-β-ketoimine ligands **1**−**5** were synthesized by the routes shown in Schemes 1 and 2, following the general progression discussed below (eqs 1 and 2). The polyglyme bridge is functionalized by first tosylating

$$\underset{\text{polyglycol}}{HO(C_2H_4O)_nC_2H_4OH} \rightarrow \underset{\text{ditosylate}}{TsO(C_2H_4O)_nC_2H_4OTs} \rightarrow \underset{\text{diamine}}{H_2N(C_2H_4O)_nC_2H_4NH_2} \quad (1)$$

$$\underset{\text{capsule ligand}}{RCOCHCR'NH(C_2H_4O)_nC_2H_4NHR'CHCRO} \xrightarrow{BaH_2} \underset{\text{barium capsule complex}}{Ba[RCOCHCR'N(C_2H_4O)_nC_2H_4NR'CHCRO]} + H_2 \quad (2)$$

the terminal hydroxyl functionalities of a commercially available polyglycol.[12] This ditosylate is then subjected to reaction with

(16) Beurskens, P. T.; Admiraal, G.; Beurskens, G.; Bosman, W. P.; Garcia-Granda, S.; Gould, R. O.; Smits, J. M. M.; Smykalla, C. *The DIRDIF program system*; Technical Report of the Crystallography Laboratory, University of Nijmegen, The Netherlands, 1992.
(17) Cromer, D. T.; Waber, J. T. *International Tables for X-ray Crystallography*; The Kynoch Press: Birmingham, England, 1974; Vol. IV, Table 2.2 A.
(18) Ibers, J. A.; Hamilton, W. C. *Acta Crystallogr.* **1964**, *17*, 781.
(19) Creagh, D. C.; McAuley, W. J. In *International Tables for X-ray Crystallography*; Wilson, A. J. C., Ed.; Kluwer Academic Publishers: Boston, 1992; Vol. C, Table 4.2.6.8, pp 219−222.
(20) Creagh, D. C.; Hubbell, J. H. In *International Tables for X-ray Crystallography*; Wilson, A. J. C., Ed.; Kluwer Academic Publishers: Boston, 1992; Vol. C, Table 4.2.4.3, pp 200−206.
(21) Zhang, J.; Gardiner, R. A.; Kirlin, P. S.; Boerstler, R. W.; Steinbeck, J. *Appl. Phys. Lett.* **1992**, *61*, 2882.

Scheme 2. Di-β-ketoiminate Ligand Syntheses of 2,2-Dimethyl-3,5-hexanedione Derivatives

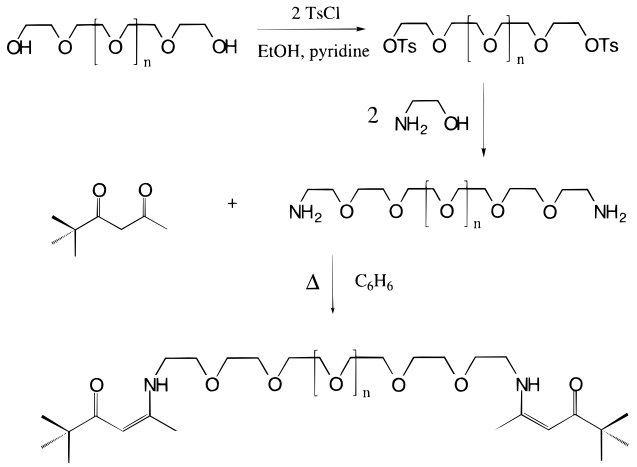

Ligand	n	Abbreviation
3	0	$H_2(dhd)_2CAP$-4
4	1	$H_2(dhd)_2CAP$-5

diethanolamine, yielding a diamine as well as lengthening the polyglyme bridge.[13] The final ligands are then assembled either by condensation of the diamine with the requisite β-diketone (Scheme 2) or by reaction of the diamine with the appropriate activated, TMS-substituted β-diketone (Scheme 1).[7m] A simple condensation reaction can be used to obtain the bridged ligand derivatives of 2,2-dimethyl-3,5-hexanedione (Hdhd; Scheme 2). However, this condensation route does not yield the corresponding dpm-derived ligand, presumably because of the greater ^{t}Bu steric encumberance.[22] The ligands derived from the more sterically hindered/less reactive dpm and hfa synthons are readily formed via the trimethylsilyl substitution route.[15] The β-diketones are commercially available, or can be straightforwardly prepared by known methods.[11] The final di-β-ketoimine ligands are purified by fractional distillation and then reacted with excess neat BaH_2 under an inert atmosphere (eq 2). This barium source offers the advantages of being highly reactive, relatively cheap, commercially available, and unreacted quantities are readily removed by filtration. After a short reaction period at 120 °C, the resulting barium complexes can be extracted with THF or heptane. However, the solubility of the complexes in heptane is relatively low, creating the need for multiple extractions. The yields of compounds **6**, **7**, and **9** were not optimized in this regard and might be increased by multiple solvent extractions as was carried out for complex **8**. Colorless or light yellow, slightly air-sensitive crystalline solids are obtained. Complexes **6** and **8** (shown in Chart 1) can be readily sublimed at 120 °C/10^{-5} Torr, while the relatively high temperature of 215 °C/10^{-5} Torr is required to sublime compound **9**.

NMR Studies. NMR data for the free di-β-ketoimine ligands and corresponding barium complexes prepared are compiled in the Experimental Section. All spectra are consistent with the proposed ligand structures and molecular connectivities. Broad singlets are observed in the ^{1}H spectra corresponding to the appropriate quantity of N−H protons for the capsule ligands. This observation confirms the preponderance of the ketoamino tautomer in $CDCl_3$ solution in agreement with earlier studies on β-ketoimines.[7n,23] The ^{1}H and ^{13}C NMR spectra of the barium complexes in C_6D_6 (or in DMSO-d_6 for less soluble **9**) at room temperature are consistent with a single stereoisomer and/or stereochemically nonrigid structures.

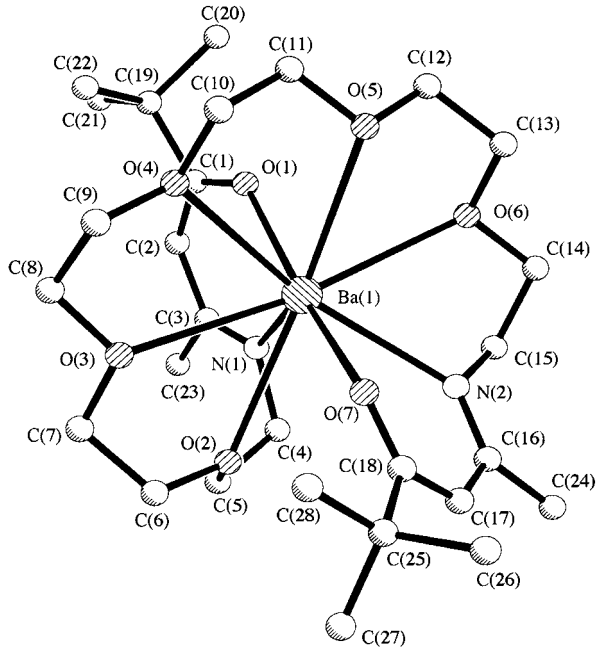

Figure 2. Single-crystal structure of the complex Ba[$(dhd)_2$CAP-5] (**8**).

Chart 1. Encapsulated Barium Complexes Discussed in the Text

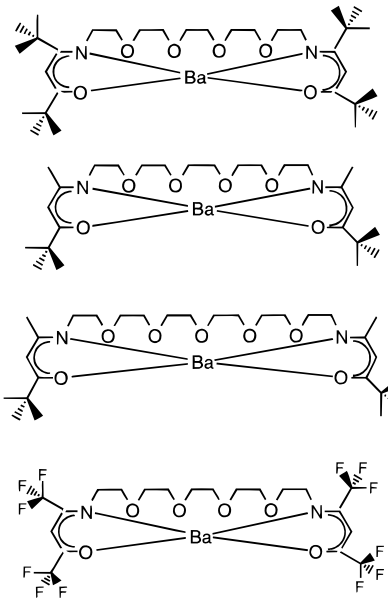

6 $Ba(dpm)_2$CAP-4

7 $Ba(dhd)_2$CAP-4

8 $Ba(dhd)_2$CAP-5

9 $Ba(hfa)_2$CAP-4

Mass Spectral Data. The electron impact mass spectroscopic data for the free ligands and their barium complexes are similar (see the Experimental Section for details). The monomeric parent ion is observed for all of the species. The major fragment usually corresponds to loss of a ^{t}Bu group. Almost all the other fragments are derived from scission of C−C or C−O bonds in the polyether bridge.

Single-Crystal Diffraction Studies. In mononuclear complexes **8** (Figure 2) and **9**·2DMSO (Figure 3), the ligand surrounds the Ba^{2+} center in an encapsulating binding mode

(22) Layer, R. W. *Chem. Rev.* **1963**, *63*, 489.

(23) Neumayer, D. A. Ph.D. Thesis, Northwestern University, Evanston, IL, 1995.

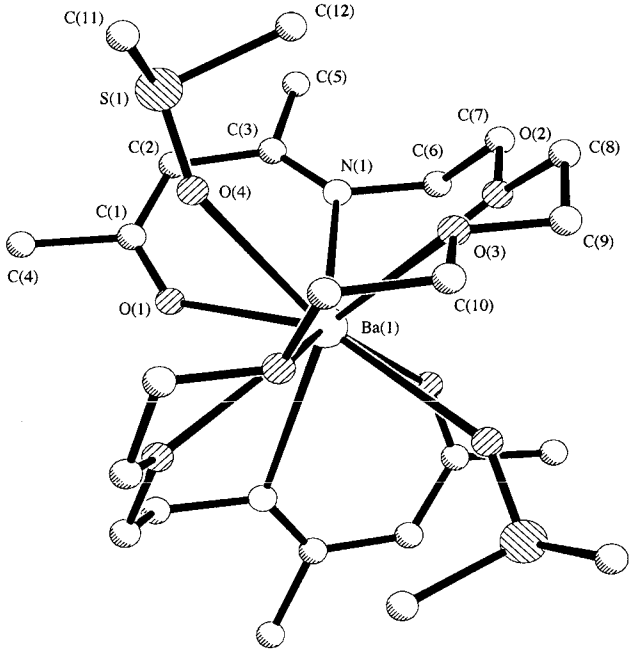

Figure 3. Single-crystal structure of the complex Ba[(hfa)$_2$CAP-4]·2DMSO (**9**·2DMSO).

Table 2. Selected Bond Lengths (Å) and Angles (deg) for Ba[(dhd)$_2$CAP-5] (**8**) and Ba[(hfa)$_2$CAP-4]·2DMSO (**9**·2DMSO)

	bond lengths (Å)	
	8	**9**·2DMSO
Ba(1)−O(1)	2.610(4)	2.647(2)
Ba(1)−O(2)	2.937(4)	2.988(2)
Ba(1)−O(3)	2.970(5)	3.061(2)
Ba(1)−O(4)	2.931(4)	2.769(3)
Ba(1)−O(5)	2.942(4)	
Ba(1)−O(6)	2.912(4)	
Ba(1)−O(7)	2.630(5)	
Ba(1)−N(1)	2.824(5)	3.026(3)
Ba(1)−N(2)	2.788(6)	

bond angles (deg) for **8**		bond angles (deg) for **9**·2DMSO	
O(1)−Ba(1)−O(2)	115.9(1)	O(1)−Ba(1)−O(1)	92.6(1)
O(1)−Ba(1)−O(3)	100.1(1)	O(1)−Ba(1)−O(2)	117.42(6)
O(1)−Ba(1)−O(4)	74.5(1)	O(1)−Ba(1)−O(2)	74.45(7)
O(1)−Ba(1)−O(5)	73.1(1)	O(1)−Ba(1)−O(3)	141.33(7)
O(1)−Ba(1)−O(6)	77.8(1)	O(1)−Ba(1)−O(3)	116.05(7)
O(1)−Ba(1)−O(7)	168.3(1)	O(1)−Ba(1)−O(4)	69.23(8)
O(1)−Ba(1)−N(1)	64.9(1)	O(1)−Ba(1)−O(4)	150.68(8)
O(1)−Ba(1)−N(2)	122.4(2)	O(1)−Ba(1)−N	61.56(7)
		O(1)−Ba(1)−N	69.14(1)

with all oxygen and nitrogen atoms coordinated to a single Ba^{2+} center. Chiral complex **8** crystallizes in centrosymmetric space group $P2_1/c$, containing both enantiomers in the unit cell. Complex **9**·2DMSO crystallizes in the space group $C2/c$ and has a 2-fold molecular symmetry axis. Ba−O/N distances in **9**·2DMSO are somewhat longer than in **8** (Table 2); however, they are similiar to those in other structurally characterized Ba(β-ketoiminate)$_2$ complexes.[7n] Ba−O(β-ketoiminate) bond distances are 2.610(4) and 2.630(5) Å in **8** and 2.647(2) Å in **9**·2DMSO. Ba−N(β-ketoiminate) bond distances are 2.787(6) and 2.824(5) Å in **8** and 3.026(3) Å in **9**·2DMSO. Ba−O(ether) bond distances range from 2.912(4) to 2.970(4) Å in **8** and from 2.988(2) to 3.061(2) Å in **9**·2DMSO. The Ba−O(DMSO) bond distance is 2.769(3) Å in **9**·2DMSO. A search of the Cambridge Structure Database did not reveal Ba−DMSO complexes for comparison. The comparatively longer bond distances in **9**·2DMSO are attributable to the larger coordination number of the Ba^{2+} center, as well as repulsive steric effects of the CF_3 moieties and DMSO ligands.

Structure of Complex 8. The geometry of **8** is similiar to that in M(β-diketonate)$_2$·polyether complexes where the coordinated polyether oxygen atoms lie in a meridional plane with β-diketonate ligands above and below the plane in an approximately orthogonal relationship.[9a,24] In **8**, the β-ketoiminate portions of the encapsulating ligand defined by O1−N1−C1−C2−C3 and O7−N2−C16−C17−C18 are planar to within 0.0157 and 0.0240 Å, respectively. The Ba^{2+} atom is displaced from the O1−N1−C1−C2−C3 and O7−N2−C16−C17−C18 planes by 0.7533 and 0.9408 Å, respectively, and the O1−Ba−N1 and O7−Ba−N2 equilateral planes are tilted from the O1−N1−C1−C2−C3 and O7−N2−C16−C17−C18 planes by 19.3° and 24.3°, respectively. The dihedral angle between the O1−Ba−N1 and O7−Ba−N2 planes is 56.1°. In contrast, the corresponding dihedral angle in Ba(hfa)$_2$·tetraglyme is 19.3°,[9a] in Ba(tfa)$_2$·tetraglyme, 21.4°,[9a] in Ba(dpm)$_2$·tetraglyme, 29.6°,[9a] and in Ba(dpm)$_2$·triglyme, 70.0°.[9a]

The five coordinated ether oxygen atoms O2, O3, O4, O5, and O6 of **8** and the Ba^{2+} ion define a meridional plane within 0.129 Å and with a Ba^{2+} displacement of 0.0763 Å from the mean-square plane. The dihedral angles between the meridional plane defined by barium and the ether oxygens and the planes defined by O1−Ba−N1 and O7−Ba−N2 are 76.4° and 83.9°, respectively.

The five coordinated polyether oxygens O2−O6 and β-ketoiminate nitrogen atom N2 define a regular hexagon with Ba^{2+} at the center. The N2 nitrogen vertex is displaced −1.0718 Å from the plane of the polyether oxygens such that the hexagon is not perfectly planar. The other β-ketoiminate nitrogen, N1, is displaced 2.163 Å from this plane. To accommodate N1, which is not part of the regular hexagon, the O2−C5−C4−N1 torsion angle (−61.7°) has the same sign as the O2−C6−C7−O3 torsion angle (−63.4°) adjacent to it. This forces the C5−O2−C6−C7 torsion angle toward gauche (−92.5°). The sequence of the remaining torsion angles is ag^+a (a = anti, g = gauche), with the gauche angle signs strictly alternating. The result is a zigzag polyether configuration, resulting in a wrapping mode coordination, typical of such complexes.[25] The overall torsion angle sequence for the β-ketoiminate nitrogens and polyether portion of the encapsulating ligand begining at O2−C5−C4−N1 and ending at O6−C14−C15−N2 is $(g^-)a{\sim}g^-(g^-)aa(g^+)aa(g^-)aa(g^+)aa(g^-)$ with the O−C−C−O(N) torsion angles in parentheses. The O−C−C−O gauche torsion angles involving the coordinated polyether oxygen atoms strictly alternate positive and range from 63.2° to 66.3°. The O2−C5−C4−N1 and O6−C14−C15−N2 torsion angles are both negative and slightly smaller at 61.7° and 61.6°, respectively.

The immediate coordination geometry about the Ba^{2+} center in **8** is distorted from an idealized tricapped trigonal prism (Figure 4). One trigonal prism triangular face is defined by O1, O5, and O6, and the capping atoms are N1, N2, and O4. The second trigonal prism triangular face is defined by O2, O3, and O7. The equilateral triangular planes defined by the vertices and the capping atoms are tilted with respect to each other, resulting in a distortion from an ideal tricapped trigonal prism. The dihedral angle between the plane defined by the capping atoms and barium and the planes defined by the vertices O1,

(24) van der Sluis, P.; Spek, A. L.; Timmer, K.; Meinema, H. A. *Acta Crystallogr.* **1990**, *C46*, 1741.
(25) Dale, J. *Isr. J. Chem.* **1980**, *20*, 3.

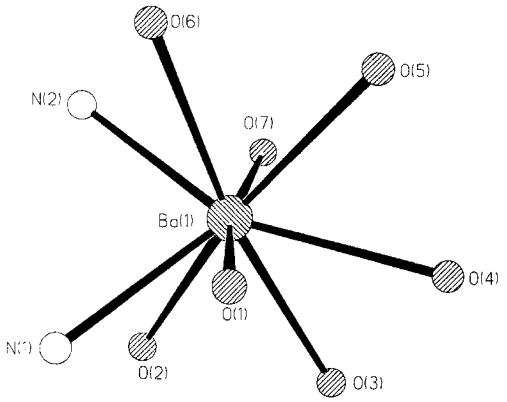

Figure 4. Immediate coordination geometry about the barium center of the complex Ba[(dhd)$_2$CAP-5] (**8**).

O5, and O6 and O2, O3, and O7 are 13.7° and 14.9°, respectively. The dihedral angle between the two trigonal planes is 8.9°. In a nondistorted tricapped trigonal prism the corresponding planes would be parallel with 0° dihedral angle. The distorted tricapped trigonal prismatic geometry in **8** is distinguished from the monocapped square antiprism geometry by the N1−Ba−O5 angle of 134° and the N1−Ba−O4 angle of 122°. The corresponding angles in an ideal tricapped trigonal prism would be 135° and 120°, and would both be equal to 127° in a monocapped square antiprism.[26]

Structure of Complex 9·2DMSO. The geometry of **9**·2DMSO is similiar to those of M(β-diketonate)$_2$·polyether complexes where the coordinated polyether oxygen atoms lie in a meridional plane with β-diketonate ligands above and below the plane in an approximately orthogonal relationship.[7j,9a,24] However, in **9**·2DMSO, the two β-diketonates which are bonded to the termini of the polyether meridional plane form the arms of an approximate "Y" around the Ba^{2+} center with the polyether meridional plane as the bottom leg and the β-ketoiminate portions the arms of the "Y". **9**·2DMSO has a C_2 axis which generates two sets of equivalent bond and plane angles. The β-ketoiminate portion of the encapsulating ligand defined by O1−N−C1−C2−C3 is planar to within 0.0462 Å, with the Ba^{2+} atom displaced from the O1−N1−C1−C2−C3 plane by 1.011 Å. The O1−Ba−N equilateral plane is tilted from the O1−N1−C1−C2−C3 plane by 24.9°, while the dihedral angle between the O1−Ba−N1 and O1a−Ba−N1a planes is 98.5°. In contrast, the dihedral angle between the corresponding planes in Ba(hfa)$_2$·tetraglyme is 19.3°,[9a] in Ba(tfa)$_2$·tetraglyme, 21.4°,[9a] in Ba(dpm)$_2$·tetraglyme, 29.6°,[9a] and in Ba(dpm)$_2$·triglyme, 70.0°.[9a]

The four coordinated ether atoms O2−O3−O2a−O3a and Ba^{2+} define a meridional plane to within 0.0052 Å, with Ba^{2+} in the mean-square plane. The dihedral angles between the meridional plane defined by Ba^{2+} and the ether oxygens and the planes defined by O1−Ba−N1 and O1a−Ba−N1a are 139.1° and 40.9°, respectively. The two DMSO ligands lie on either side of the meridional plane defined by the coordinated polyether oxygen atoms with O4(DMSO) +2.5505 Å from the mean-square plane. The four coordinated polyether O atoms and the two β-ketoiminate N atoms define a regular hexagon with an O or N atom at each vertex and Ba^{2+} at the center. The two adjacent β-ketoimiate nitrogen vertexes are displaced +1.437 Å out of plane defined by the coordinated polyether oxygens such that the hexagon is not perfectly planar. That portion of the ligand from N1 to N1a adopts essentially the same conformation as a D_{3d} 18-crown-6: the C−O−C−C torsion angles are all anti and the O−C−C−O torsion angles alternate g^+, with the gauche angle signs strictly alternating. The result is a zigzag polyether configuration, resulting in a wrapping mode of coordination, typical of such complexes.[25]

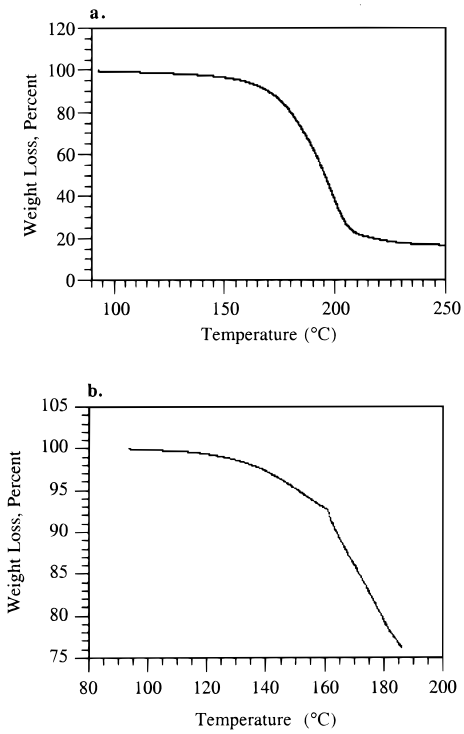

Figure 5. (a) Thermogravimetric analysis data for Ba[(dhd)$_2$CAP-5] (**8**) at 6.0 Torr under nitrogen with a temperature ramp of 5 °C·min^{-1}. (b) Thermogravimetric analysis data for Ba[(dpm)2CAP-4] (**6**) at 6.0 Torr under nitrogen with a temperature ramp of 5 °C·min^{-1}.

Precursor Vapor Transport Properties. Vacuum thermogravimetric analytical data for the nonfluorinated compounds Ba[(dhd)$_2$CAP-5] (**8**) and Ba[(dpm)$_2$CAP-4] (**6**) are shown in Figure 5. Samples were examined at 6.0 Torr under N_2, with a temperature ramp rate of 5 °C/min. Ba[(dhd)$_2$CAP-4] (**7**) decomposes before it reaches sublimation temperature and is therefore not included in these measurements. The fluorinated compound Ba[(hfa)$_2$CAP-4] (**9**) does not sublime until 215 °C/10^{-5} Torr, well above nonfluorinated compounds **6** and **8**, as well as many previously reported fluorinated ligand compounds.[7i,24,27] TGA data were collected on complexes **6** and **8** because they are the most volatile (readily sublime at temperatures as low as 100 °C/10^{-5} Torr with negligible residue). Ba[(dhd)$_2$CAP-5] (**8**) exhibits a steady weight loss with the >80% of the sample volatilized by 220 °C. This large percentage weight loss is important because the decomposition temperature of the compound is ~220 °C as evidenced by an exotherm in the DSC data. For the compound to sublime without decomposition, the sublimation temperature should be maintained well below the decomposition temperature. Unfortunately, although Ba[(dpm)$_2$CAP-4] (**6**) is volatile under isothermal sublimation, under the temperature-ramped TGA conditions only ~10% sublimes before the onset decomposition temperature of 160 °C is reached. Therefore, any CVD process with this precursor must necessarily operate below 160 °C. If the process were operated near or above the decomposition temperature, the vapor pressure of the compound would fall over the course

(26) Favas, M. C.; Kepert, D. C. *Prog. Inorg. Chem.* **1981**, *28*, 67.

(27) Timmer, K.; Spee, C. I. M. A.; Mackor, A.; Meinema, H. A.; Spek, A. L.; van der Sluis, P. *Inorg. Chim. Acta* **1991**, *190*, 109.

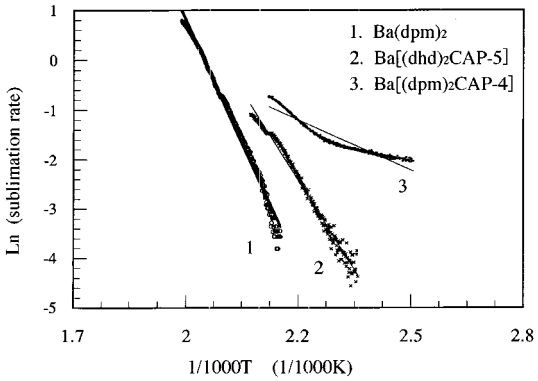

Figure 6. Arrhenius plots of the sublimation rate vs temperature for barium capsule compounds Ba[(dpm)$_2$CAP-4] (**6**) and Ba[(dhd)$_2$CAP-5 (**8**), and Ba(dpm)$_2$. The straight lines are drawn as a guide to the eye.

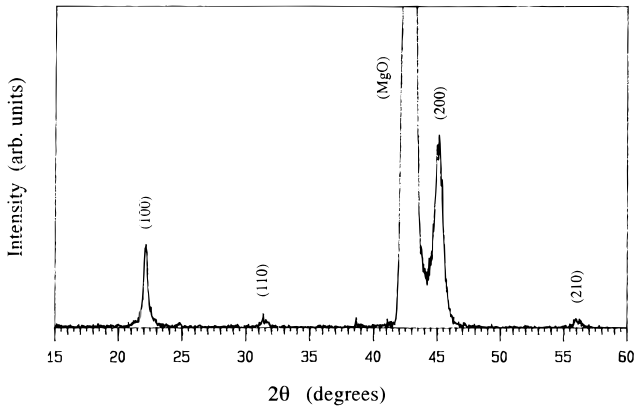

Figure 7. Θ−2Θ X-ray diffraction spectrum of a $BaTiO_3$ thin film grown on (001) MgO by MOCVD from Ba[(dhd)$_2$CAP-5] (**8**) and Ti(dpm)$_2$(O^{i}Pr)$_2$.

of the film deposition, causing stoichiometry fluctuations in the film, and irreproducible growth characteristics. The data show that Ba[(dhd)$_2$CAP-5] (**8**) is substantially more thermally stable and therefore potentially a better MOCVD source than Ba[(dpm)$_2$CAP-4] (**6**).

The Arrhenius plots of ln(sublimation rate) vs 1/*T* shown in Figure 6 compare the volatility of complexes **6** and **8** to that of Ba(dpm)$_2$. These plots, corrected for diffusion distance by methods discussed previously,[6g] clearly demonstrate the enhanced volatility of the present capsule complexes over that of Ba(dpm)$_2$. This enhanced volatility reasonably arises from the reduced nuclearity (Ba(dpm)$_2$ is a cluster[8e,d]), stronger chelation, and increased steric bulk of the capsule ligand over two dpm ligands. As noted in the crystal structure discussion, the present complexes are monomeric, with the ligand completely filling the Ba^{2+} coordination sphere. The enhanced volatility is similar to what is observed in monomeric Ba(dpm)$_2$·(Lewis base) complexes. However, as confirmed in the TGA of Ba[(dhd)$_2$CAP-5] (**8**), the Lewis base does not/cannot dissociate as in Ba(dpm)$_2$·(Lewis base) complexes,[9a,b] reflecting the stronger bonding expected of the covalently linked polyether ligand component.[28] The present capsule complexes have greater connectivity of the coordinating elements than the Ba(dpm)$_2$· polyglyme counterparts, which is qualitatively expected to afford greater coordinative and thermal stability. This effect is observed in many ligand systems other than glymes[29] such as cryptands,[30] substituted cyclopentadienyls,[31] ethylene derivatives,[31,32] and silyl and phosphino ligands,[33] affording qualitatively/quantitatively more stable complexation.[34] Variations on this ligand architecture to further increase connectivity are likely to enhance the volatility and thermal stability of this class of barium−organic complexes even further.

There are marked differences in volatilities and stabilities among the Ba^{2+} complexes synthesized in this study which likely originate from a combination of differences in molecular structure and intermolecular interactions. The surprisingly modest volatility of the fluorinated complex Ba[(hfa)$_2$CAP-4] (**9**) may be due to intermolecular bonding. The crystal structure shows that the extra coordination sites of **9** are filled by two DMSO molecules. In the case of thermal DMSO loss, these coordination sites might well be taken up by other molecules, creating oligomers with reduced volatility. The nonfluorinated complexes appear to have volatility characteristics which are more dependent on the individual molecular structures than on intermolecular interactions. In fact, the concern with the nonfluorinated complexes is more one of thermal stability than volatility. The stabilities appear to be dependent on intramolecular steric characteristics of the ligand. The most thermally stable complex (**8**) does not appear to have unusually adverse intramolecular steric interactions as discussed in the crystal structure section above. However, when all the β-ketoimine methyl groups are replaced with tertiary butyl groups (as was attempted in the reaction of H$_2$(dpm)$_2$CAP-5) (**2**) with BaH_2), the ligand does not form a Ba^{2+} complex under the synthetic conditions employed, presumably a steric consequence. Conversely, the lack of tertiary butyl groups in **7** likely does not afford as stable encapsulation as in **6**. Although the volatility and stability of these ligands can be qualitatively understood in terms of structural properties, they have fewer possible conformations than ligands coordinated to Ba^{2+} compounds with multiple unconnected bidentate ligands. The trends are qualitatively reminiscent of the marked ligand structure−metal ion binding selectivities observed for polyethers.[35] Clearly steric interactions play a significant role in maximizing the stability of Ba^{2+} coordination by these encapsulating ligands.

$BaTiO_3$ Film Growth Studies. $BaTiO_3$ films were grown by MOCVD to demonstrate the utility of the present capsule compounds as CVD sources for barium. The films were grown by low-pressure MOCVD using Ba[(dhd)$_2$CAP-5] (**8**) and Ti(dpm)$_2$(O^{i}Pr)$_2$ (see the Experimental Section for details) with O_2 and N_2O as the oxidizer gases. The similar lattice constants of MgO ($a = b = 3.99$ Å, $c = 4.04$ Å) and $BaTiO_3$ ($a = b = c = 4.21$ Å) ensure a relatively small mismatch of 5.4%.

The colorless thin films deposited were clear or slightly cloudy. Due to the cloudy appearance of the MgO substrate, it

(28) Cotton, F. A.; Wilkinson, G. *Advanced Inorganic Chemistry, 5th ed.*; John Wiley and Sons: New York, 1988; pp 45−47.
(29) (a) Arunasalam, V.-C.; Baxter, I.; Drake, S. R.; Hursthouse, M. B.; Abdul Malik, K. M.; Miller, S. A. S.; Mingos, D. M. P.; Otway, D. J. *J. Chem. Soc., Dalton Trans.* **1997**, 1331. (b) Bahl, A. M.; Krishnaswamy, S.; Massand, N. G.; Burkey, B. J.; Hanusa, T. P. *Inorg. Chem.* **1997**, *36*, 5413.
(30) (a) Chand, D. K.; Bharadwaj, P. K. *Inorg. Chem.* **1996**, *35*, 3380. (b) Lehn, J. M.; Sauvage, J. P. *J. Am. Chem. Soc.* **1975**, *97*, 6700.
(31) Zimmermann, K. H.; Pilato, R. S.; Horvath, I. T.; Okuda, J. *Organometallics* **1992**, *11*, 3935.
(32) Aizawa, S.; Matsuda, K.; Tajima, T.; Maeda, M.; Sugata, T.; Funahashi, S. *Inorg. Chem.* **1995**, *34*, 2042.
(33) Schubert, U.; Gilges, H. *Organometallics* **1996**, *15*, 2373.
(34) (a) Dwyer, F. P.; Mellor, D. P. *Chelating Agents and Metal Chelates*; Academic Press: New York, 1964; pp 42−47. (b) Martell, A. E.; Calvin, M. *Chemistry of the Metal Chelate Compounds*; Prentice Hall: Englewood Cliffs, NJ, 1952; pp 143−149.
(35) (a) Rogers, R. D.; Bond, A. H.; Roden, D. M. *Inorg. Chem.* **1996**, *35*, 6964. (b) Rogers, R. D.; Jezl, M. L.; Bauer, C. B. *Inorg. Chem.* **1994**, *33*, 5682. (c) Nazarenko, A. Y.; Pyantnitskii, I. V. *Zh. Neorg. Khim.* **1987**, *32*, 1006.

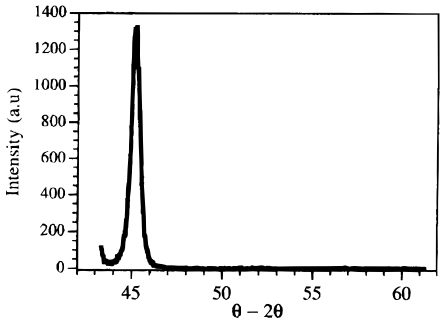

Figure 8. X-ray diffraction ω-scan rocking curve of the (200) reflection of an MOCVD-derived $BaTiO_3$ film indicating a full width at half-maximum value of 1.10°.

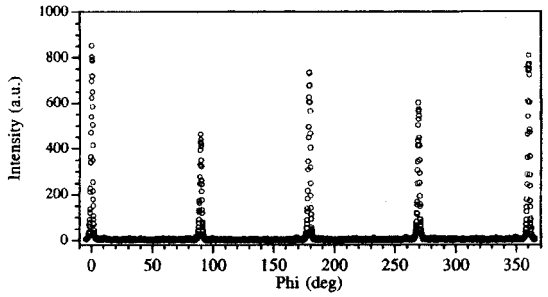

Figure 9. In plane ϕ-scan of the (220) reflection of an MOCVD-derived $BaTiO_3$ film grown on (001) MgO showing epitaxial cubic growth.

is difficult to determine if the cloudy appearance arises solely from the substrate or if there is a contribution from the film. SEM studies evidence a smooth, featureless film surface. Energy-dispersive X-ray microanalysis (EDX) shows the presence of Ba and Ti in an average atomic ratio of 1:1. The $\theta-2\theta$ X-ray diffraction pattern in Figure 7 shows that the film consists of a $BaTiO_3$ perovskite phase oriented in the [l00] direction;[36] i.e., the film is highly oriented with the *a*-axis perpendicular to the MgO substrate. The growth plane alignment is further evidenced by the relatively narrow ω-scan rocking curve which has a full width at half-maximum of 1.10° for the $BaTiO_3$ (200) reflection (Figure 8). An in-plane ϕ-scan (Figure 9) shows the relative film orientation with respect to the substrate $a-b$ plane. Reflections appear every 90° as expected for an epitaxial, tetragonal $BaTiO_3$ film.

(36) Wills, L. A.; Wessels, B. W.; Richeson, D. S.; Marks, T. J. *Appl. Phys. Lett.* **1992**, *60*, 41.

Conclusions

A class of fluorine-free barium β-ketoiminate complexes containing a new chelating ligand class have been prepared for use as MOCVD precursors. The new ligand, consisting of two β-ketoiminate ligands covalently connected by a polyether linker, provides an encapsulating polyether girdle and two tethered anionic bidentate functionalities. The coordination sphere of the Ba^{2+} is filled by these ligands via eight or nine coordinative bonds. Both nonfluorinated and fluorinated ligands have been prepared and characterized. The nonfluorinated complexes Ba[$(dhd)_2$CAP-5] (**8**) and [$Ba(dpm)_2$CAP-4] (**6**) are substantially more volatile than $Ba(dpm)_2$ according to sublimation characteristics and vacuum TGA analysis. Thin epitaxial films of $BaTiO_3$ were grown with Ba[$(dhd)_2$CAP-5] (**8**) to demonstrate the promise of this class of compounds as MOCVD precursors.

The major benefit of the present ligand system is a reduction in the tendency for oligomerization compared to the traditional source, $Ba(dpm)_2$, thus enhancing volatility. Since the two β-diketonate ligands of $Ba(dpm)_2$ only provide four formal coordination sites, the Ba^{2+} forms oligomeric species of increased coordination number. The present ligand systems offer eight or nine interconnected binding sites, thereby impeding oligomerization. Furthermore, the single ligand capsule system exhibits enhanced thermal stability over these complexes having two or three separate ligands per barium. The outlook for this new class of ligands shows much promise. Although not all ligands synthesized here readily form Ba^{2+} complexes, presumably due to steric constraints, there are many possibilities for new derivatives. Work in our laboratory is continuing in this direction.

Acknowledgment. This work was supported by the NSF Science and Technology Center for Superconductivity (Grant DMR91-2000) and by the NSF (Grant CHE98-07042). Characterization facilities of the Northwestern Materials Research Center were supported by the NSF MRSEC program (Grant DMR96-32472). We thank Drs. R. McNeely and J. Belot of Northwestern University and Dr. J. Zhang and Mr. Tom Baum of Adanced Technology Materials, Inc. for experimental assistance. D.B.S. thanks Adanced Technology Materials, Inc. for a student research internship.

Supporting Information Available: Tables of crystallographic details, complete atomic coordinates and *U* values, distances and angles, and anisotropic displacement parameters. This material is available free of charge via the Internet at http://pubs.acs.org.

IC991161A